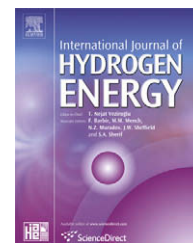


Available at www.sciencedirect.comjournal homepage: www.elsevier.com/locate/he

Ion transport resistance in Microbial Electrolysis Cells with anion and cation exchange membranes

Tom H.J.A. Sleutels^{a,b}, Hubertus V.M. Hamelers^{a,*}, René A. Rozendal^c, Cees J.N. Buisman^{a,b}

^aSub-Department of Environmental Technology, Wageningen University, Bomenweg 2, P.O. Box 8129, 6700 EV Wageningen, The Netherlands

^bWetsus, Centre of Excellence for Sustainable Water Technology, Agora 1, P.O. Box 1113, 8900 CC Leeuwarden, The Netherlands

^cAdvanced Water Management Centre (AWMC), The University of Queensland, Qld 4072, Australia

ARTICLE INFO

Article history:

Received 13 January 2009

Received in revised form

27 February 2009

Accepted 1 March 2009

Available online 1 April 2009

Keywords:

MEC

Ion exchange membrane

MFC

Internal resistance

Hydrogen

ABSTRACT

Previous studies have shown that Microbial Electrolysis Cells (MECs) perform better when an anion exchange membrane (AEM) than when a cation exchange membrane (CEM) separates the electrode chambers. Here, we have further studied this phenomenon by comparing two analysis methods for bio-electrochemical systems, based on potential losses and partial system resistances. Our study reconfirmed the large difference in performance between the AEM configuration ($2.1 \text{ m}^3 \text{ H}_2 \text{ m}^{-3} \text{ d}^{-1}$) and CEM configuration ($0.4 \text{ m}^3 \text{ H}_2 \text{ m}^{-3} \text{ d}^{-1}$) at 1 V. This better performance was caused mainly by the much lower internal resistance of the AEM configuration ($192 \text{ m}\Omega \text{ m}^2$) compared to the CEM configuration ($435 \text{ m}\Omega \text{ m}^2$). This lower internal resistance could be attributed to the lower transport resistance of ions through the AEM compared to the CEM caused by the properties of both membranes. By analyzing the changes in resistances the limitations in an MEC can be identified which can lead to improved cell design and higher hydrogen production rates.

© 2009 International Association for Hydrogen Energy. Published by Elsevier Ltd. All rights reserved.

1. Introduction

Because of concern of depletion of fossil fuels and the threat of global warming, the search for green energy sources strengthens [1]. A possible green energy source is the chemical energy from organic waste [2]. Bio-electrochemical conversion of organic compounds is a novel technology that can efficiently capture this energy and is therefore a topic with increasing research interest [3]. One of the most promising emerging bio-electrochemical technologies is hydrogen production in a Microbial Electrolysis Cell (MEC) [4–6]. MECs convert the chemical energy of the wastewater into hydrogen gas and at the same time purify the wastewater by degrading the organic compounds [7]. MECs contain two electrodes: an anode and a cathode. At the anode electrochemically active micro-organisms oxidize the organic compounds to protons,

CO₂ and electrons. The electrons are released to the anode and move through an electrical circuit to the cathode [8,9]. In the cathode of an MEC the electrons are used to reduce water to hydrogen gas [10,11]. For this reduction reaction theoretically only a small amount of energy (0.12 V) is needed which can be added by means of a power supply [4].

To compensate for the negative charge (electrons) moving from anode to cathode, ions move through an ion selective membrane [12–14]. Typically cation exchange membranes have been used for this purpose, but several studies have now shown that MEC configurations with an anion exchange membrane (AEM) outperform those with a cation exchange membrane (CEM) [11,13,15].

The objective of this study was to further elucidate the reasons for the large difference in performance between MECs with a CEM and an AEM. For this purpose we have developed

* Corresponding author. Tel.: +31 317 483447; fax: +31 317 482108.

E-mail address: bert.hamelers@wur.nl (H.V.M. Hamelers).

an analysis method based on partial system resistances. The partial system resistance can be calculated by dividing the potential loss of every part of the system by the current density ($R = V/j$). At a constant applied voltage the current density that is produced by MECs depends on the internal resistance of the system. Detailed analysis of this internal resistance can give additional information about different systems to the comparison of potential losses. With this analysis method the performance of different systems, for example with a CEM and an AEM, can be compared and explained in detail. Furthermore, different experimental conditions, e.g. changes during an experimental run, can be compared. Comparison of these partial resistances can reveal the limitations in the system for optimization. In the future this can lead to improved cell design and higher hydrogen production rates.

2. Materials and methods

2.1. Electrochemical cell

Experiments were performed in two electrochemical cells similar to the cell used in [16], where the liquid flows in serpentine fashion parallel to the electrodes through a flow channel. Only in this set-up the width of the flow channel was 1.7 cm (was 1.5 cm) and the channel depth was 0.8 cm (was 1 cm) creating an anode and a cathode chamber both of 280 mL. This flow channel is used to press the electrodes onto the membrane, which separates the anode and cathode chamber. Two types of ion exchange membranes (surface area 250 cm²) were used: (i) a cation exchange membrane (Fumasep[®] FKE, FuMa-Tech GmbH, Germany) and (ii) an anion exchange membrane (Fumasep[®] FAA, FuMa-Tech GmbH, Germany). Both the anode and the cathode chamber were equipped with an Ag/AgCl reference electrode (+0.20 V against NHE – ProSense QiS, Oosterhout, The Netherlands) connected to the cell through a Haber–Luggin capillary. The anode was made of graphite felt (projected surface area 0.025 m², thickness 6.5 mm – National Electrical Carbon BV, Hoorn, The Netherlands). The cathode was made of a platinum coated (50 g m⁻²) titanium mesh (projected surface area 250 cm², thickness 1 mm, specific surface area 1.7 m² m⁻² – Magneto Special Anodes BV, Schiedam, The Netherlands). The electrodes were connected to a power supply (ES 03-5, Delta Electronica BV, Zierikzee, The Netherlands).

2.2. Experimental procedures

The anode chamber was continuously fed with synthetic wastewater (pH 7) at a rate of 5 mL min⁻¹. This synthetic wastewater consisted of 1.36 g L⁻¹ NaCH₃COO·3H₂O, 0.74 g L⁻¹ KCl, 0.58 g L⁻¹ NaCl, 0.68 g L⁻¹ KH₂PO₄, 0.87 g L⁻¹ K₂HPO₄, 0.28 g L⁻¹ NH₄Cl, 0.1 g L⁻¹ MgSO₄·7H₂O, 0.1 g L⁻¹ CaCl₂·2H₂O and 0.1 mL L⁻¹ of a trace element mixture [17]. To minimize differences in mass-transfer losses between the two electrochemical configurations, acetate was always available in excess to ensure no substrate limitations occurred. Each electrochemical cell was started up by inoculating the anode with 100 mL of effluent from an active MEC [13]. After current

production had stabilized, hydrogen production was studied in duplicate runs of 48 h. Before every run the cathode was flushed with 10 mM of potassium phosphate buffer and subsequently filled with exactly 750 mL (electrode compartment + circulation volume) of the same buffer solution (pH 7). This flushing of the cathode resulted in a neutral pH in the cathode and limited the pH gradient over the membrane at the start of an experimental run. To remove oxygen the cathode was flushed with N₂ gas (purity >99.9%). The anode was flushed with influent until the pH was 7. A run was started by closing the electrical circuit to apply a voltage of 1 V. During a run hydrogen gas accumulated in the head-space of the cathode and gas left the system through a gas flow meter (Milligascounter[®], Ritter, Bochum, Germany). The hydrogen fraction in this flow was determined every 12 h by gas chromatography according to [11]. The anode was sampled every 12 h and analyzed for acetate content using ion chromatography (Metrohm 761 Compact IC equipped with a conductivity detector and a Metrosep Organic Acids 6.1005.200 ion exclusion column). Ion content of anolyte and catholyte was determined at the start and end of a yield test using a total organic carbon analyzer (Shimadzu TOC-VCPH) for carbonate, an ion chromatograph (Metrohm 761 Compact IC) equipped with a conductivity detector and an anion column (Metrosep A Supp 5 6.1006.520) for other anions (Cl⁻, NO₂⁻, NO₃⁻, PO₄³⁻, and SO₄²⁻), a standardized test kit for ammonium (ammonium cuvette test LCK303, XION 500 spectrophotometer, Dr. Lange Nederland B.V., The Netherlands) and inductively coupled plasma-optical emission spectroscopy (ICP-OES—Perkin Elmer Optima 3000XL) for other cations (Na⁺, K⁺, Ca²⁺, and Mg²⁺). Total charge production in the form of electrons was compared to the transport of charge in the form of these specific ions according to [11].

A data logger (Memo-graph, Endress + Hauser) continuously logged 8 variables for both cells: anode and cathode potential and cell voltage, current, anode and cathode pH (Liquisys M CPM 253, Endress + Hauser), anode and cathode conductivity (ProSense QiS, Oosterhout, The Netherlands). Conductivity and pH for anode and cathode were measured in a flow cell through which the anolyte/catholyte was continuously pumped at a rate of 340 mL min⁻¹. Measured pH values at high salt concentrations can deviate because of liquid junction potentials and were therefore corrected using the measured ion concentrations. The temperature was kept constant at 303 K.

2.3. Calculations

The applied voltage (E_{cell}) can be divided in two parts: (i) a reversible energy loss and (ii) an irreversible energy loss. The first part of the applied voltage consists of the energy used to overcome the thermodynamical barrier of hydrogen production (equilibrium voltage; E_{eq}). This energy input is recovered in hydrogen gas and is therefore a reversible energy loss. The equilibrium voltage was calculated at pH 7 because this is the pH of the anolyte and catholyte at the start of an experimental run. This way a distinction can be made between the reversible and irreversible energy input. The equilibrium voltage

was calculated using the Nernst equation with the actual concentrations of acetate and bicarbonate using

$$E_{\text{eq}} = E_{\text{cat}} - E_{\text{an}} = \left(E_{\text{cat}}^0 - \frac{RT}{2F} \ln \frac{p\text{H}_2}{[10^{-7}]^2} \right) - \left(E_{\text{an}}^0 - \frac{RT}{8F} \ln \frac{[\text{CH}_3\text{COO}^-]}{[\text{HCO}_3^-]^2 [10^{-7}]^9} \right) \quad (1)$$

where E_{cat} is the theoretical cathode potential (V), E_{an} is the theoretical anode potential (V), E_{cat}^0 is the standard cathode potential (V), E_{an}^0 is the standard anode potential (V), R is the universal gas constant ($8.3145 \text{ J mol}^{-1} \text{ K}^{-1}$), T is the temperature (303 K) and F is the Faraday's constant (96485 C mol^{-1}).

The second part of the applied voltage is the irreversible energy loss. This energy is lost as a result of the resistances of different parts of the cell. This voltage loss consists of (i) the pH gradient over the membrane ($E_{\Delta\text{pH}}$), (ii) anode overpotential (η_{an}), (iii) cathode overpotential (η_{cat}), (iv) ionic losses (E_{ionic}) and (v) transport losses (E_{T}) [18]

$$E_{\text{cell}} = E_{\text{cmf}} - E_{\Delta\text{pH}} - \eta_{\text{an}} - \eta_{\text{cat}} - E_{\text{ionic}} - E_{\text{T}} \quad (2)$$

The ohmic loss other than the ionic losses of the electrolyte was not measured separately and is included in the overpotential of the anode and cathode [13]. During an experimental run a pH gradient develops over the membrane which gives an extra amount of potential loss [19]. This pH gradient loss (V) over the membrane was calculated with

$$E_{\Delta\text{pH}} = \frac{RT}{F} \ln \left(10^{(\text{pH}_{\text{cathode}} - \text{pH}_{\text{anode}})} \right) \quad (3)$$

The anode and cathode overpotential (V) was calculated with

$$\eta_{\text{an}} = E_{\text{an,measured}} - E_{\text{an}}, \quad \eta_{\text{cat}} = E_{\text{cat}} - E_{\text{cat,measured}} \quad (4)$$

where $E_{\text{an,measured}}$ is the measured anode potential and $E_{\text{cat,measured}}$ is the measured cathode potential. The anode and cathode overpotentials were calculated using the actual concentrations of acetate, bicarbonate and protons at the start and at the end of a run (48 h) (Equation (1)). The anode and cathode overpotential includes the mass-transfer and charge transfer overpotential and in case of the anode overpotential also the potential that is used by the micro-organisms for growth and maintenance. The ionic loss (V) is related to the electrolyte resistance of the anolyte and catholyte and was estimated with [12]

$$E_{\text{ionic}} = I_{\text{ions}} \left(\frac{1}{2} R_{\text{an}} + \frac{1}{2} R_{\text{cat}} \right) = I_{\text{ions}} \left(\frac{d_{\text{an}}}{2A\sigma_{\text{an}}} + \frac{d_{\text{cat}}}{2A\sigma_{\text{cat}}} \right) \quad (5)$$

where I_{ions} is the flow of ions through the electrolyte (A m^{-2}) which is equal to the current density, d_{an} is the distance between the anode and the membrane (m), d_{cat} is the distance between the cathode and the membrane (m), A is the surface area (m^2), σ_{an} is the anode conductivity (S m^{-1}) and σ_{cat} is the cathode conductivity (S m^{-1}). The factor 1/2 is included to estimate the location of the biomass and where the charge is produced inside the felt.

The transport loss (E_{T}) was calculated from all other potential losses using equation (2). The transport loss is the potential loss caused by transport of ions through the membrane. The transport loss can also be calculated as the difference between the reference electrode of the anode

and the reference electrode of the cathode corrected for the ionic resistance of both anolyte and catholyte and the membrane pH gradient [12]. Both methods have been used to calculate the transport resistance during the entire experimental period and the values obtained from both calculation methods correspond.

To calculate the potential losses several parameters should be measured in order to be able to perform the calculations: anode and cathode potential, pH and conductivity, the cell voltage and the produced current density.

2.4. MEC performance

The performance of an MEC can be described by the volumetric performance and the energetic performance. The volumetric performance is the amount of hydrogen gas that is produced ($\text{m}^3 \text{ H}_2 \text{ m}^{-3} \text{ d}^{-1}$) and the energetic performance is the amount of electrical energy that is required per m^3 of hydrogen. Total gas production was measured during a yield test to calculate the volumetric hydrogen production rate. The amount of captured hydrogen can be related to the amount of current produced in the cathodic efficiency. The cathodic efficiency is calculated from the produced current and the measured amount of hydrogen ($V_{\text{H}_2}^{\text{meas}}; L$) [11]

$$\eta_{\text{cat}} = \frac{V_{\text{H}_2}^{\text{meas}} 2F}{V_{\text{m}} \int_{t=0}^t I dt} \quad (6)$$

where V_{m} is the molar gas volume (22.4 L mol^{-1}).

3. Results and discussion

3.1. MEC performance

In this study we tried to further elucidate the difference in performance of an MEC equipped with an AEM and an MEC equipped with a CEM by looking at changes in potential losses and internal resistance during an experimental run. The performance of both systems was studied in duplicate runs of 48 h (Table 1). At the start of an experimental run the pH in both the anode and the cathode was 7. Due to electron transport ions are transported through the membrane. Because ions other than hydroxyl and protons are present in the electrolyte a pH gradient develops over the membrane [13]. Fig. 1A shows the development of this membrane pH gradient and Fig. 1B shows the development of the current density for both configurations during an experimental run. The current density shows that the configuration with the AEM outperforms the CEM ($\text{CEM } 2.3 \text{ A m}^{-2}$; $\text{AEM } 5.3 \text{ A m}^{-2}$).

Table 1 – Comparison of the performance of two MECs equipped with a CEM and an AEM at an applied voltage of 1 V.

	Current density (A m^{-2})	Cathodic efficiency (%)	Hydrogen production ($\text{m}^3 \text{ H}_2 \text{ m}^{-3} \text{ d}^{-1}$)
CEM	2.3 ± 0.3	47 ± 6	0.4 ± 0.1
AEM	5.3 ± 0.5	83 ± 13	2.1 ± 0.5

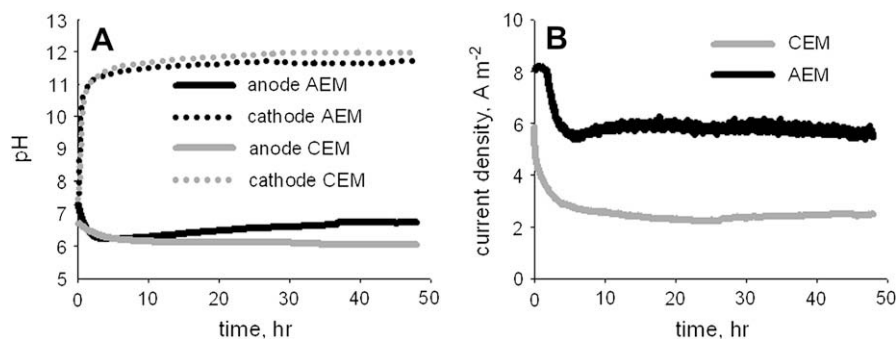


Fig. 1 – Development of the pH (A) in anode and cathode and current density (B) in MECs equipped with an AEM and a CEM during a 48 h experimental run at an applied voltage of 1 V.

The higher bio-electrochemical performance of a system equipped with an AEM compared to a system equipped with a CEM is in accordance with results reported in previous research [13,15]. The hydrogen production rate for the AEM configuration ($2.1 \text{ m}^3 \text{ H}_2 \text{ m}^{-3} \text{ d}^{-1}$) is higher compared to the CEM configuration ($0.4 \text{ m}^3 \text{ H}_2 \text{ m}^{-3} \text{ d}^{-1}$). This hydrogen production rate for the AEM configuration was high compared to other studies where continuous systems were used (Rozendal et al. [13] $1.1 \text{ m}^3 \text{ H}_2 \text{ m}^{-3} \text{ d}^{-1}$ ($V_{\text{cell}} = 1 \text{ V}$); Tartakovsky et al. [20] $0.92 \text{ m}^3 \text{ H}_2 \text{ m}^{-3} \text{ d}^{-1}$ ($V_{\text{cell}} = 1.26 \text{ V}$) and Ditzig et al. [21] $0.01 \text{ m}^3 \text{ H}_2 \text{ m}^{-3} \text{ d}^{-1}$ ($V_{\text{cell}} = 0.5 \text{ V}$)). However, hydrogen production rates of these continuous systems are lower than the hydrogen production rates reported for small batch systems (Call and Logan [22] $3.12 \text{ m}^3 \text{ H}_2 \text{ m}^{-3} \text{ d}^{-1}$ ($V_{\text{cell}} = 0.8 \text{ V}$) and Cheng and Logan [15] $1.23 \text{ m}^3 \text{ H}_2 \text{ m}^{-3} \text{ d}^{-1}$ ($V_{\text{cell}} = 0.6 \text{ V}$)).

The cathodic efficiency was higher in the AEM configuration (83%) than in the CEM configuration (47%). Together with the higher current density in the AEM configuration compared to the CEM configuration this higher cathodic efficiency explains the higher hydrogen production rate. The cathodic efficiencies found in this study are low compared to previous studies (101% for both CEM and AEM [11]). Part of the hydrogen is lost due to diffusion through the membrane and through the extensive tubing used in the circulation of the catholyte [23]. The relative amount of hydrogen lost due to diffusion however is higher at lower hydrogen production rates [4]. This explains the higher cathodic efficiency in the AEM configuration compared to the CEM configuration which had a lower hydrogen production rate.

3.2. Potential losses

An overview of the calculated potential losses (equations (1)–(5)) at the end of a yield test for both membrane configurations is shown in Fig. 2A. These potential losses consist of: (i) equilibrium voltage, (ii) pH gradient, (iii) anode overpotential, (iv) cathode overpotential, (v) ionic losses and (vi) transport losses. This figure shows that at the end of a yield test for the CEM configuration (current density 2.3 A m^{-2}) most potential was lost in the pH gradient over the membrane (0.36 V) and the transport loss through the membrane (0.29 V). For the AEM configuration (current density 5.3 A m^{-2}) the anode overpotential (0.33 V) and the pH gradient over the membrane (0.30 V) were the largest losses at the end of a yield test. By

comparing the potential losses it does not become clear however why the AEM configuration outperforms the CEM configurations because for both MEC configurations the total potential loss is equal to the applied voltage. This is different from MFCs where the cell voltage is lower when some parts of the system have a higher potential loss [24]. In MECs it is therefore not possible to compare the performance of different systems by looking at the potential losses. Comparison of potential losses in MECs is only possible at the same current densities since the total potential loss is current dependent. Within one system on the other hand, it is possible to determine what part is limiting the performance by looking at the potential losses.

3.3. Resistances

Compared to the potential losses the internal resistance can give additional information about the performance of an MEC, especially when comparing different systems [18,25]. Since the voltage needed for hydrogen production is constant, the current density depends on the total internal resistance of the system, which in itself is a function of the current density. The total internal resistance is a sum of the partial resistances of the system [25]. The partial resistances were calculated by dividing the calculated potential loss by the current density ($R = V/j$). The current density was used here to calculate the resistance instead of the current. This way the resistance is expressed independently of reactor size ($\Omega \text{ m}^2$) which makes comparison between different reactor systems possible. Some researchers prefer to express resistances and currents as volumetric measures [26]. However, the current density depends on the active surface of the electrode material. The projected surface area of the anode will eventually be the dominant parameter for scaling up of the system [27]. For these reasons it is decided here to express the resistance as a measure of the projected surface area.

At the end of a yield test the total resistance of the AEM configuration was $192 \text{ m}\Omega \text{ m}^2$ while the total resistance of the CEM configuration was $435 \text{ m}\Omega \text{ m}^2$. To explain the differences in performance of the AEM and CEM configuration a more detailed analysis of this internal resistance is necessary. Therefore the partial internal resistances were calculated (Fig. 2B). These partial resistances consist of: (i) equilibrium resistance, (ii) pH gradient resistance, (iii) anode resistance,

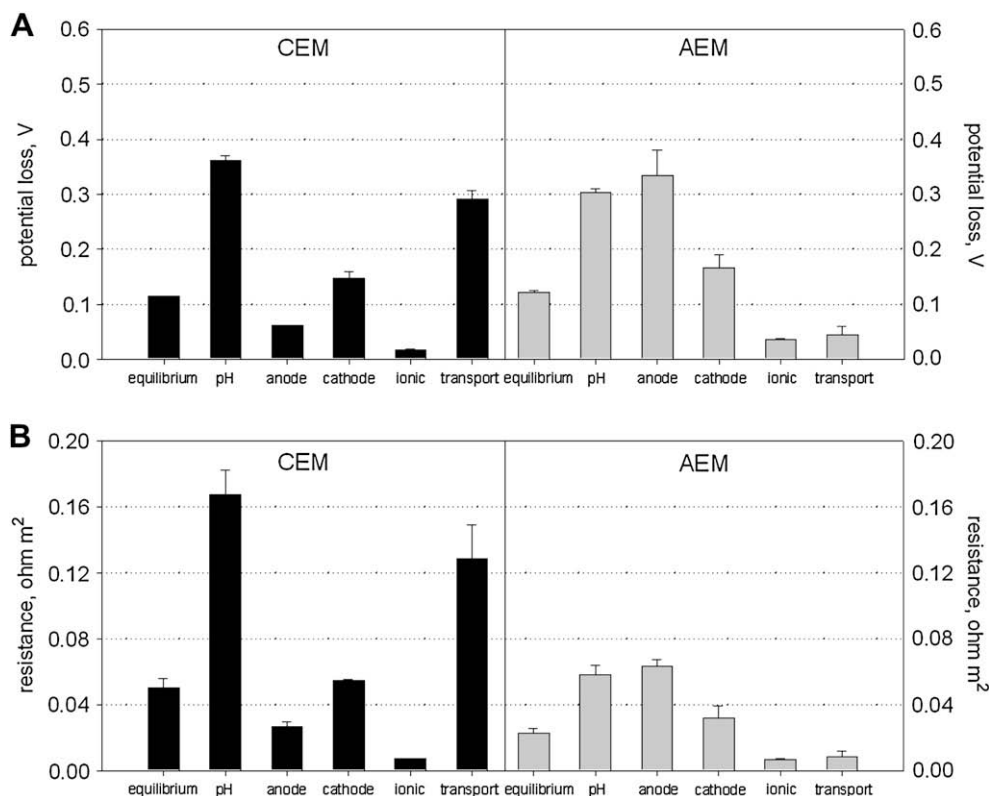


Fig. 2 – Comparison of potential losses (A) and resistances (B) in MECs equipped with a CEM (2.3 A m^{-2}) and an AEM (5.3 A m^{-2}) at the end of a yield test at an applied voltage of 1 V.

(iv) cathode resistance, (v) ionic resistance and (vi) transport resistance. Fig. 3 gives an overview of these partial internal resistances in an MEC, which can be represented by a series of resistances in an equivalent circuit.

When we compare the potential losses in Fig. 2A and the internal resistances in Fig. 2B it becomes clear that the ratio of potential losses and resistances for one configuration is the same. However, there are also differences between the potential losses and internal resistances between the two configurations. When we compare the resistances for both systems it immediately becomes clear that the total resistance of the AEM configuration is lower than the total resistance of the CEM configuration.

Furthermore, when we compare the potential losses and partial resistances for the two different membrane configurations some differences in conclusions exist. For example, the cathode potential loss in the CEM configuration (0.15 V) is smaller than the cathode potential loss in the AEM configuration (0.17 V) while the cathode resistance for the CEM configuration is larger ($65 \text{ m}\Omega \text{ m}^2$) than the cathode resistance for the AEM configuration ($32 \text{ m}\Omega \text{ m}^2$).

The main differences between analysis of internal resistances and analysis of potential losses are: (i) the internal resistances of the different parts of the system can be quantified and compared to the internal resistances of another system, e.g. a comparison between a configuration with a CEM and a configuration with an AEM can be made and (ii) it is possible to compare different experimental conditions within one system, e.g. it is possible to compare the start of an

experimental run with the end of an experimental run. This comparison of resistances is possible because the resistances are normalized to the current densities and most potential losses are current dependent. Comparison of potential losses gives more information when current independent parameters like the equilibrium voltage are compared.

3.4. Transport resistance

One of the most striking differences between the two membrane configurations is the transport resistance. This transport resistance is the resistance experienced by the ions that are transported through the membrane. The concentration of ions in anolyte and catholyte changes during an experimental run and therefore also the transport resistance changes during an experimental run (Fig. 4). Since the comparison of the partial resistances is independent of current density it is also possible to compare different experimental conditions. Therefore it is also possible to compare the transport resistance at the start of an experimental run to the transport resistance at the end of an experimental run. At the start of an experimental run anolyte and catholyte composition for both membrane configurations was comparable. Still the transport resistance of the CEM configuration ($48 \text{ m}\Omega \text{ m}^2$) was already much higher than the transport resistance in the AEM configuration ($12 \text{ m}\Omega \text{ m}^2$). At the end of an experimental run this difference in transport resistance between CEM ($128 \text{ m}\Omega \text{ m}^2$) and AEM configuration ($8 \text{ m}\Omega \text{ m}^2$) became only larger.

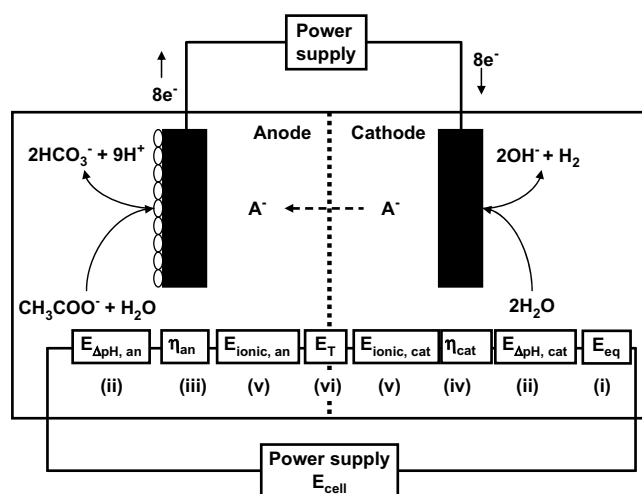


Fig. 3 – Overview of the potential losses in an MEC equipped with an AEM at an applied voltage of 1 V. The potential losses consist of: (i) equilibrium voltage, (ii) pH gradient, (iii) anode overpotential, (iv) cathode overpotential, (v) ionic losses and (vi) transport losses. Both the pH gradient and the ionic losses can be split up in an anodic and a cathodic part. The total internal resistance of an MEC can be represented as a series of resistances in an equivalent circuit. The total potential loss is always equal to the applied voltage (E_{cell}).

From Fig. 1A it seems as if at the end of an experimental run the pH in both the anode and cathode chamber and the current density become constant. This suggests that a significant part of the charge transport was represented by hydroxyl and/or protons. Since hydroxyl and protons are closely linked to buffer components through the water equilibrium it is difficult to distinguish between the transport of hydroxyl, protons and buffer components. Fig. 5 shows the conductivity in the cathode as a function of the transported charge through the system during a typical experimental run. This figure confirms that the ion concentration in the cathode of the AEM configuration is already going to equilibrium and the dominant species transported here will be hydroxyl and/or protons

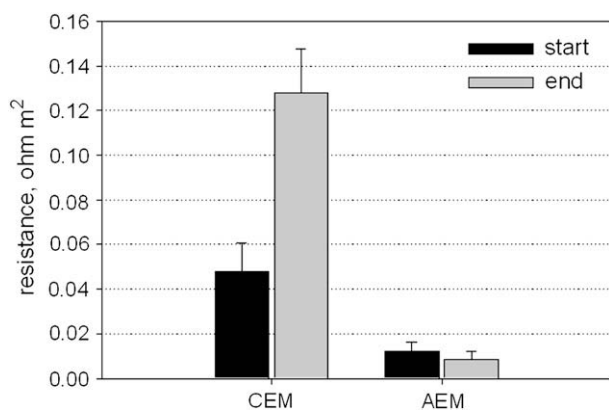


Fig. 4 – Transport resistance at the start and end of an experimental run in an MEC equipped with an AEM and in an MEC equipped with a CEM.

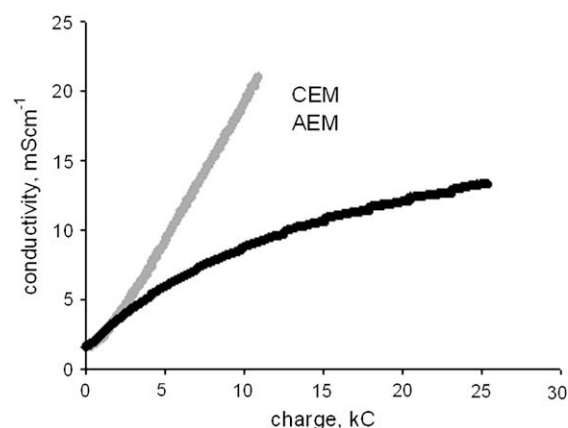


Fig. 5 – Conductivity of the cathode as a function of the produced charge during an experimental run.

and buffer components. The conductivity in the cathode of the CEM configuration, however, still increases linearly. This implies that still other ions than protons and hydroxyl are being transported through the membrane and the pH is not constant. Fig. 6 shows an overview of the contribution of ions present in the system to the total charge transport through the membrane during the total experimental runs. Because no distinction can be made between transport of protons and hydroxyl through measurements the transport of H^+/OH^- was calculated from the total transport of electrons and the total transport of all other ions [13]. This figure confirms that in the AEM configuration hydroxyl and protons represent most charge transport through the membrane. For the CEM configuration hydroxyl and protons also form the largest fraction of charge transport, but also other, especially cations, take part in charge transport.

The transport of the type of ion depends on the concentration difference between the anode and cathode compartment for that specific ion. However, because the membrane is charged, counter-ions will move into the membrane to compensate for this charge. As a result, the concentration of ions inside the membrane will be significantly different from

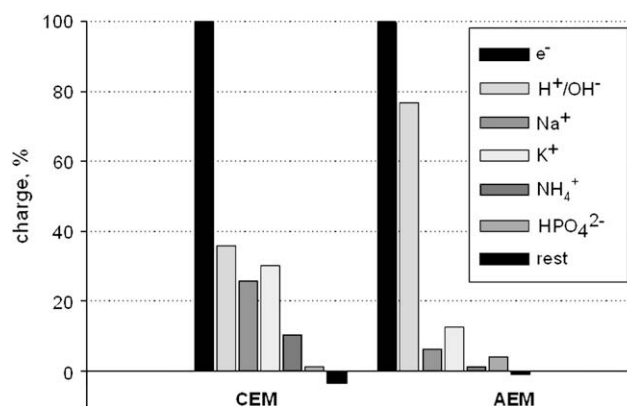


Fig. 6 – Comparison of the total charge production (e^-) to the transport of specific ions through CEM and AEM in an experimental run at an applied voltage of 1.0 V. Total charge production is set to 100% for relative comparison.

the concentration of ions in the solutions and also the actual concentration gradient for those ions will be different. The concentration gradient of ions inside the membrane can be calculated with the Donnan equilibrium [28]. This Donnan equilibrium gives the relation between the concentration of ions in the electrolyte (C_{ion} in mol L⁻¹) and the concentration of ions in the membrane (\bar{C}_{ion} in mol L⁻¹)

$$K_{\text{Donnan}} = \frac{\bar{C}_{\text{ion}}}{C_{\text{ion}}} \quad (7)$$

The Donnan equilibrium depends on the charge inside the membrane and is represented by the fixed charge density. This fixed charge density (C_{fix} in mol L⁻¹) is the amount of charge the membrane contains per liter and can be calculated from the concentration of ion exchange groups attached to the polymer matrix (IEC; mequiv g_{dry}⁻¹) and the swelling degree (SD; $g_{\text{H}_2\text{O}} g_{\text{dry}}^{-1}$) [29]. To maintain electroneutrality, the charge inside the membrane will be compensated by ions from the electrolyte. The composition of the total charge moving into the membrane depends on the composition of the electrolyte. The ratio of ions in the electrolyte and ions in the membrane is represented as the Donnan equilibrium as shown by equation (7).

With this Donnan equilibrium the concentration gradient for the most important ions contributing to ion transport was calculated for both membrane configurations at the start and end of an experimental run. Table 2 shows an overview of the estimated concentration gradients inside the CEM and AEM.

Table 2 – Estimation of most important ion concentration gradients inside cation and anion exchange membranes with the Donnan equilibrium at the start and end of an experimental run. A positive gradient corresponds to a higher anode concentration compared to the cathode concentration.

	CEM		AEM	
	Start	End	Start	End
IEC (mequiv g ⁻¹)	1.36 ^a		1.5 ^b	
SD (%)	12 ^a		25 ^b	
C_{fix} (mol L ⁻¹)	11.3		6.0	
Ion concentration (mol L ⁻¹)	Start	End	Start	End
K ⁺	-0.60	-4.9	0	-0.004
Na ⁺	0.23	-2.9	0	-0.002
Ca ²⁺	0.097	2.8	0	0
Mg ²⁺	0.03	0.95	0	0
Cl ⁻	0	0	0.77	0.77
SO ₄ ²⁻	0	0	0.30	0.24
NH ₄ ⁺	0.12	0.26	0	0
Acetate ⁻	0	0	0.16	0.018
HCO ₃ ⁻	0	0	0.046	0.17
H ₂ PO ₄ ⁻	0	0	0.097	0.25
HPO ₄ ²⁻	0	0	-0.84	1.6
PO ₄ ³⁻	0	0	0	-1.6
H ⁺	0	0	0	0
OH ⁻	0	-0.006	0	-0.07

a Data taken from Dlugolecki et al. [29].

b Data taken from technical datasheet FuMa-Tech GmbH, Germany [30].

From this table it becomes clear that at the start of an experimental run the largest concentration gradients are represented by K⁺, Na⁺, NH₄⁺, Mg²⁺ and Ca²⁺ in the CEM. The concentration gradient for K⁺ is -0.60 mol L⁻¹. This negative concentration means that the concentration of K⁺ in the cathode is higher than the concentration in the anode. Fig. 6 shows that K⁺ contributes to a large part (30%) of the charge transport through the membrane although they are transported against their concentration gradient. Transport of ions against a concentration gradient will give a larger resistance for transport. At the end of the experimental run the concentration gradient for K⁺ and also Na⁺ is even more negative (-4.9 and -2.9 mol L⁻¹ respectively). The increase in transport resistance at the end of the experimental run compared to the start of the experimental run corresponds to this increase in ion concentration in the membrane. Furthermore the concentration gradient at the end of an experimental run for Ca²⁺ is large (2.8 mol L⁻¹) while hardly any Ca²⁺ is transported through the membrane as can be seen from Fig. 6. It is likely that Ca²⁺ does contribute to the charge transport but precipitated together with phosphate or carbonate in the cathode compartment.

In the AEM configuration the concentration gradients for the different phosphate buffer species show the most interesting results. At the start of an experimental run especially HPO₄²⁻ is transported from the cathode to the anode, while some other species are transported back. At the end of an experimental run the concentration gradient for HPO₄²⁻ is 1.6 mol L⁻¹ while the concentration gradient for PO₄³⁻ is -1.6 mol L⁻¹. This means PO₄³⁻ is transported to the anode while HPO₄²⁻ is transported back to the cathode. This causes shuttling of charge through buffer species that are transported through the membrane. The transport of charge through an AEM through buffer species was also suggested by Cheng and Logan [15]. From Fig. 6 it becomes clear that in the AEM H⁺/OH⁻ contribute to a large extent (77%) to the charge transport through the membrane. However, H⁺/OH⁻ are closely linked to buffer species through the water equilibrium and it is therefore hard to distinguish between these species. So the transport of buffer species through the membrane is actually also transport of H⁺/OH⁻ through the membrane.

For both membranes it is worth mentioning that the concentration gradient for protons is negligible and protons will therefore hardly contribute to charge transport through the membrane. The differences in transport resistance for both membranes are caused by the properties of the membrane and the concentration gradients these properties cause inside the membrane.

The calculated transport resistance in the AEM configuration (8 mΩ m²) is much higher than the membrane resistance alone (<0.2 mΩ m² [30]). Besides transport losses through the membrane, the transport of ions could also be limited by the anode configuration. In the set-up used, the anode material is pressed against the membrane creating an anolyte layer inside the felt that is not well mixed. Visual inspection of the anode clearly showed that the major part of the biofilm was growing on the anolyte side of the graphite felt. Therefore the charge transport in the AEM configuration has to move from the membrane through the felt towards the biofilm. Ion transport limitations are especially evident in systems with

low alkalinity and ionic strength like the system used in this study [31,32]. These low buffer concentrations were used in this study because eventually the system will be applied in the treatment of wastewater. Wastewater also has a low buffer capacity, so here ion transport will also become a problem.

In this study we presented two methods to analyze MEC systems in detail and to compare different experimental stages. These methods are based on the calculation of the partial internal resistances and potential losses of the system. Comparison of the partial resistances of an MEC equipped with a CEM and with an AEM showed that the AEM configuration outperforms the CEM configuration because of a much lower transport resistance. In the future the calculation of the partial internal resistances can be used to quantify changes in internal resistance and to identify limitations in the system. Reduction of specific internal resistances can in the future lead to better cell design and higher hydrogen production rates. Because the resistances are expressed as $\Omega \text{ m}^2$ they are independent of reactor size and can be compared for every cell type.

Acknowledgements

This work was performed in the TTIW-cooperation framework of Wetsus, Centre of Excellence for Sustainable Water Technology (www.wetusus.nl). Wetsus is funded by the Dutch Ministry of Economic Affairs, the European Union European Regional Development Fund, the Province of Fryslan, the city of Leeuwarden and by the EZ-KOMPAS Program of the “Samenwerkingsverband Noord-Nederland”. The authors like to thank the participants of the research theme “Hydrogen” for the fruitful discussions and their financial support. The authors further thank Annemiek ter Heijne and David Strik for critical reading of the manuscript. René Rozendal is supported by the Australian Research Council (DP 0666927).

REFERENCES

- [1] Faaij APC. Bio-energy in Europe: changing technology choices. *Energy Policy* 2006;34:322–42.
- [2] Angenent LT, Karim K, Al-Dahhan MH, Wrenn BA, Domiguez-Espinosa R. Production of bioenergy and biochemicals from industrial and agricultural wastewater. *Trends in Biotechnology* 2004;22:477–85.
- [3] Logan BE, Hamelers B, Rozendal R, Schröder U, Keller J, Freguia S, et al. Microbial fuel cells: methodology and technology. *Environmental Science & Technology* 2006;40:5181–92.
- [4] Rozendal RA, Hamelers HVM, Euverink GJW, Metz SJ, Buisman CJN. Principle and perspectives of hydrogen production through biocatalyzed electrolysis. *International Journal of Hydrogen Energy* 2006;31:1632–40.
- [5] Liu H, Grot S, Logan BE. Electrochemically assisted microbial production of hydrogen from acetate. *Environmental Science & Technology* 2005;39:4317–20.
- [6] Logan BE, Call D, Cheng S, Hamelers HVM, Sleutels THJA, Jeremiasse AW, et al. Microbial electrolysis cells (MECs) for high yield hydrogen gas production from organic matter. *Environmental Science & Technology* 2008;42:8630–40.
- [7] Rozendal RA, Hamelers HVM, Rabaey K, Keller J, Buisman CJN. Towards practical implementation of bioelectrochemical wastewater treatment. *Trends in Biotechnology* 2008;26:450–9.
- [8] Lovley DR. Bug juice: harvesting electricity with microorganisms. *Nature Reviews Microbiology* 2006;4:497–508.
- [9] Bond DR, Lovley DR. Electricity production by *Geobacter sulfurreducens* attached to electrodes. *Applied and Environmental Microbiology* 2003;69:1548–55.
- [10] El-Deab MS, El-Shakre ME, El-Anadoulou BE, Ateya BG. Electrolytic generation of hydrogen on Pt-loaded porous graphite electrodes from flowing alkaline solutions. *Journal of Applied Electrochemistry* 1996;26:1133–7.
- [11] Rozendal RA, Hamelers HVM, Molenkamp RJ, Buisman CJN. Performance of single chamber biocatalyzed electrolysis with different types of ion exchange membranes. *Water Research* 2007;41:1984–94.
- [12] Ter Heijne A, Hamelers HVM, De Wilde V, Rozendal RA, Buisman CJN. A bipolar membrane combined with ferric iron reduction as an efficient cathode system in microbial fuel cells. *Environmental Science & Technology* 2006;40:5200–5.
- [13] Rozendal RA, Sleutels THJA, Hamelers HVM, Buisman CJN. Effect of the type of ion exchange membrane on performance, ion transport, and pH in biocatalyzed electrolysis of wastewater. *Water Science and Technology* 2008;57:1757–62.
- [14] Kim JR, Cheng S, Oh SE, Logan BE. Power generation using different cation, anion, and ultrafiltration membranes in microbial fuel cells. *Environmental Science & Technology* 2007;41:1004–9.
- [15] Cheng S, Logan BE. Sustainable and efficient biohydrogen production via electrohydrogenesis. *Proceedings of the National Academy of Sciences of the United States of America* 2007;104:18871–3.
- [16] Rozendal RA, Jeremiasse AW, Hamelers HVM, Buisman CJN. Hydrogen production with a microbial biocathode. *Environmental Science & Technology* 2008;42:629–34.
- [17] Zehnder AJB, Huser BA, Brock TD, Wuhrmann K. Characterization of an acetate-decarboxylating, non-hydrogen-oxidizing methane bacterium. *Archives of Microbiology* 1980;124:1–11.
- [18] Fan Y, Sharbrough E, Liu H. Quantification of the internal resistance distribution of microbial fuel cells. *Environmental Science & Technology* 2008;42:8101–7.
- [19] Rozendal RA, Hamelers HVM, Buisman CJN. Effects of membrane cation transport on pH and microbial fuel cell performance. *Environmental Science & Technology* 2006;40:5206–11.
- [20] Tartakovskiy B, Manuel MF, Neburchilov V, Wang H, Guiot SR. Biocatalyzed hydrogen production in a continuous flow microbial fuel cell with a gas phase cathode. *Journal of Power Sources* 2008;182:291–7.
- [21] Ditzig J, Liu H, Logan BE. Production of hydrogen from domestic wastewater using a bioelectrochemically assisted microbial reactor (BEAMR). *International Journal of Hydrogen Energy* 2007;32:2296–304.
- [22] Call D, Logan BE. Hydrogen production in a single chamber microbial electrolysis cell lacking a membrane. *Environmental Science & Technology* 2008;42:3401–6.
- [23] Chae K-J, Choi M-J, Lee J, Ajayi FF, Kim IS. Biohydrogen production via biocatalyzed electrolysis in acetate-fed bioelectrochemical cells and microbial community analysis. *International Journal of Hydrogen Energy* 2008;33:5184–92.
- [24] Rabaey K, Verstraete W. Microbial fuel cells: novel biotechnology for energy generation. *Trends in Biotechnology* 2005;23:291–8.
- [25] Bard AJ, Faulkner LR. *Electrochemical methods: fundamentals and applications*. New York: John Wiley & Sons; 2001.

- [26] Clauwaert P. Minimizing losses in bio-electrochemical systems: the road to applications. *Applied Microbiology and Biotechnology* 2008;79:901–13.
- [27] Ramasamy RP, Ren Z, Mench MM, Regan JM. Impact of initial biofilm growth on the anode impedance of microbial fuel cells. *Biotechnology and Bioengineering* 2008;101:101–8.
- [28] Sata T. Ion exchange membranes: preparation, characterization, modification and application. Cambridge: Royal Society of Chemistry; 2004.
- [29] Dlugolecki P, Nymeijer K, Metz S, Wessling M. Current status of ion exchange membranes for power generation from salinity gradients. *Journal of Membrane Science* 2008;319:214–22.
- [30] FuMa-Tech GmbH, Germany. Technical datasheet FAA ion exchange membrane; 2005.
- [31] Rozendal RA, Hamelers HVM, Rabaey K, Keller J, Buisman CJN. Towards practical implementation of bioelectrochemical wastewater treatment. *Trends in Biotechnology* 2008;26:450–9.
- [32] Liu H, Cheng SA, Logan BE. Power generation in fed-batch microbial fuel cells as a function of ionic strength, temperature, and reactor configuration. *Environmental Science & Technology* 2005;39:5488–93.